Theor Chem Acc (2009) 124:95–103
DOI 10.1007/s00214-009-0586-0

REGULAR ARTICLE

Chloromethane and dichloromethane decompositions inside nanotubes as models of reactions in confined space

Bartosz Trzaskowski · Ludwik Adamowicz

Received: 14 February 2009 / Accepted: 8 May 2009 / Published online: 29 May 2009

Abstract A combination of ab initio MP2 and molecular mechanics UFF calculations have been employed to study chloromethane and dichloromethane decomposition reaction inside carbon nanotubes (CNTs). The results suggest that the impact of the nanotubes on the mechanism of the reaction depends on the diameter of the nanotube. Nanotubes with a large diameter affect the reaction in a negligible way. On the other hand, most of the reactions taking place inside small nanotubes are considerably altered. The presence of the CNT may affect the geometries of the reactants, the reaction energy barriers, as well as the energetic outcome of the reactions. All the reactions have been described by means of energetic, thermodynamic, and vibrational analyses, which allowed us to form general conclusions concerning the reaction taking place in a confined space.

Keywords Chemical reactions · Nanotubes · Entropy · Transition state

Electronic supplementary material The online version of this article (doi:10.1007/s00214-009-0586-0) contains supplementary material, which is available to authorized users.

B. Trzaskowski · L. Adamowicz
Department of Chemistry, University of Arizona, Tucson, AZ 85721, USA

L. Adamowicz
e-mail: ludwik@u.arizona.edu

Present Address:
B. Trzaskowski (✉)
Materials and Process Simulation Center, California Institute of Technology, Pasadena, CA 91125, USA
e-mail: trzask@wag.caltech.edu

1 Introduction

Recently, there has been considerable interest in the chemical reaction taking place inside carbon nanotubes (CNTs). The nanotube confinement may have a large impact on the course of the reaction, i.e. by altering the relative energies of products, transition states, and substrates or even leading to new synthetic routes, not available without the presence of CNTs due to the unique physical and chemical properties of nanotubes. However, to date only several experimental studies concerning this problem have been presented. For example, it was demonstrated experimentally that CNTs may be used as reaction vessels for the $C_{60}O$ polymerization to yield a linear polymer $(C_{60}O)_n$ [1]. Earlier, a different study presented evidence that unsubstituted fullerenes may also undergo chemical reactions inside the CNTs that cause linear chains to form [2]. In a recent paper, Pan et al. [3] investigated a number of reactions over CNT-confined catalysts.

The theoretical research on this interesting topic has produced only a limited number of studies. In the first paper on this subject, Halls et al. [4] investigated the impact of the presence of nanotubes on the the Menshutkin S_N2 reaction. More recently, two simple reactions ($H + H_2$ and $D + H_2$ exchange reaction) have been described using quantum mechanics and classical trajectory methods [5, 6]. Additionally, density functional studies of energetic and structural properties of Fe_3C clusters and N_2 molecules have been performed recently [7, 8].

These studies, while describing interesting examples, provide a rather limited view on the effect of CNT confinement (and the confinement in general) on the reaction paths. The use of theoretical methods for studies of these types of reactions seems particularly valuable.

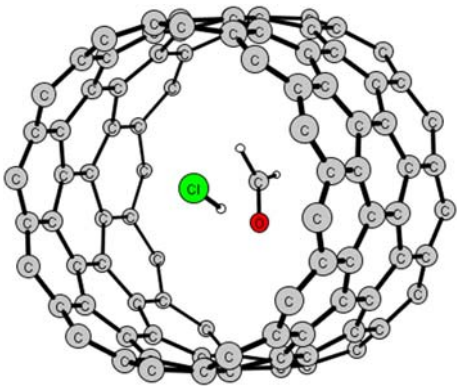

Fig. 1 A schematic representation of one of the products of the decomposition reaction encapsulated into carbon nanotube

The computational approach may provide a relatively fast, yet accurate way to describe the systems of interest and help in drawing more general conclusions concerning the reaction mechanisms. The implications of this work may have an impact on designing specific CNT systems for drug delivery [9] and engineering CNT-based reaction vessels for multiple types of chemical reactions. They also may be useful to shed more light on the general rules concerning the encapsulation of reactants.

The reactions selected for this study include decompositions of chloromethanol, dichloromethanol, and formyl chloride. The chemistry of those compounds in gas phase and in the presence of water is fairly well understood [10–12]. These compounds are of interest to environmental chemistry as chlorinated hydrocarbons have recently become frequent pollutants of drinking water supplies [13–18]. The decomposition of chlorinated hydrocarbons with and without the presence of water may be facilitated by the use of highly reactive radicals obtained from hydrogen peroxide or ozone. A better understanding of their chemistry is highly desirable due to the abundance of chlorinated hydrocarbons and their negative impact on health of living organisms.

In this work, we have performed a detailed analysis of selected reactions taking place inside CNTs of different diameters (Fig. 1). We have analyzed their reaction paths both in isolation and inside CNTs of three different diameters. The reactions have been described in terms of the enthalpies and entropies of reactants, transition states, and products for each case. The investigation sheds more light on the mechanics of the reactions when they occur inside the CNTs. It is also an important step in better understanding the general impact of the confined space on reactions. This, in the future, may allow us to better predict the course of the reaction in such an environment.

2 Models and computational details

In this study, we have investigated three different reaction paths for decomposition of chloromethanol, dichloromethanol, and formyl chloride. To describe the first process, we have used the following two reactions [12]:

$$CH_2(OH)Cl \rightarrow HCHO + HCl \quad (1)$$

and

$$HCHO + H_2O \rightarrow CH_2(OH)_2. \quad (2)$$

The second type of reaction path represents the decomposition of dichloromethanol, which may be described using the following set of reactions:

$$CH(OH)Cl_2 \rightarrow ClCHO + HCl \quad (3)$$

and

$$ClCHO \rightarrow CO + HCl. \quad (4)$$

The decomposition of dichloromethanol may also proceed via a different mechanism, described using the following three reactions:

$$CH(OH)Cl_2 + H_2O \rightarrow ClCHO + H_2O + HCl, \quad (5)$$

$$ClCHO + H_2O \rightarrow CH(Cl)(OH)_2, \quad (6)$$

and

$$CH(Cl)(OH)_2 + H_2O \rightarrow HCOOH + HCl + H_2O. \quad (7)$$

For all seven reactions, structures of the reactants (RC), the transitions states (TS), and the products (PC) have been fully optimized without any symmetry constraints. In the first step, all the geometries were calculated using the Møller–Plesset perturbation theory method, MP2 [19], with the standard 6–31+G* basis set. In the next step, the systems were placed inside three different CNTs: (8,0)-nanotube (with the diameter of 6.4 Å), (10,0)-nanotube (7.8 Å in diameter), and (12,0)-nanotube (9.4 Å in diameter). The diameter of these nanotube models is similar to the diameter of typical nanotubes used in experimental nanoscience. We have used short CNTs of $\sim$7 Å to accelerate the calculations. The use of longer nanotube models ($\sim$11 Å, see Table 4 in electronic supplementary materials) had a minor impact on the obtained results. For each reaction the system of interest was placed in the center of the nanotube in a random orientation and was fully optimized using the ONIOM approach [20, 21]. For selected systems, different orientations of the reactants were chosen to test whether the final result depends on the starting geometry. This procedure resulted in multiple minima with slightly different geometries for some systems; in such case, we have chosen systems with the lowest energy as final minima. The ONIOM method allowed us to divide the system into two layers treated with

different computational methods. We have applied the MP2/6–31+G* method to describe the chlorinated hydrocarbon system and the molecular mechanics UFF force-field method [22] to describe the CNTs.

The UFF force-field method, while simple, was shown to be adequate for isolated CNTs [23, 24]. However, the method includes only the van der Waals forces and does not describe the large electronic polarizability of the nanotubes, which is likely to be an important factor affecting the stability of the reactants and the products of an reaction that occurs insight the nanotube. The impact of polarizable nanotube may be particularly important for systems with large dipole moments, as those studied in this work [4]. This method diminishes also the impact of encapsulated molecules on the nanotube, which may undergo deformation upon interactions with reactants. Therefore, these simulations more closely approximate substrates encapsulated by organic or lipid-like system. Nevertheless, even without the polarization effects, this study of the effects of a molecular confinement on chemical reactants bring some interesting points that are common to both highly polarizable encapsulating systems, as well as to systems with a low electronic polarizability.

For each optimized structure, the Hessian matrix was calculated in order to assess whether the predicted molecular geometry corresponds to a true minimum or a transition state. The procedure allowed us to obtain a total of 84 stationary points. All calculations have been performed in the Gaussian 03 software suite [25].

3 Results and discussion

The relative energies for all three reaction paths are presented in Fig. 2. The calculated thermodynamic parameters of these paths are presented in Tables 1 and 2. The optimized structures of all reactants, transition states and products, and their orientations inside the nanotubes are presented in a schematic way in the electronic supplementary materials of this publication (Figs. 3–9). These figures also show the key geometrical parameters of the systems. All presented results are compared to the results of an earlier computational study on these systems [12], which employed MP2 perturbation theory and the 6–31+G** basis set.

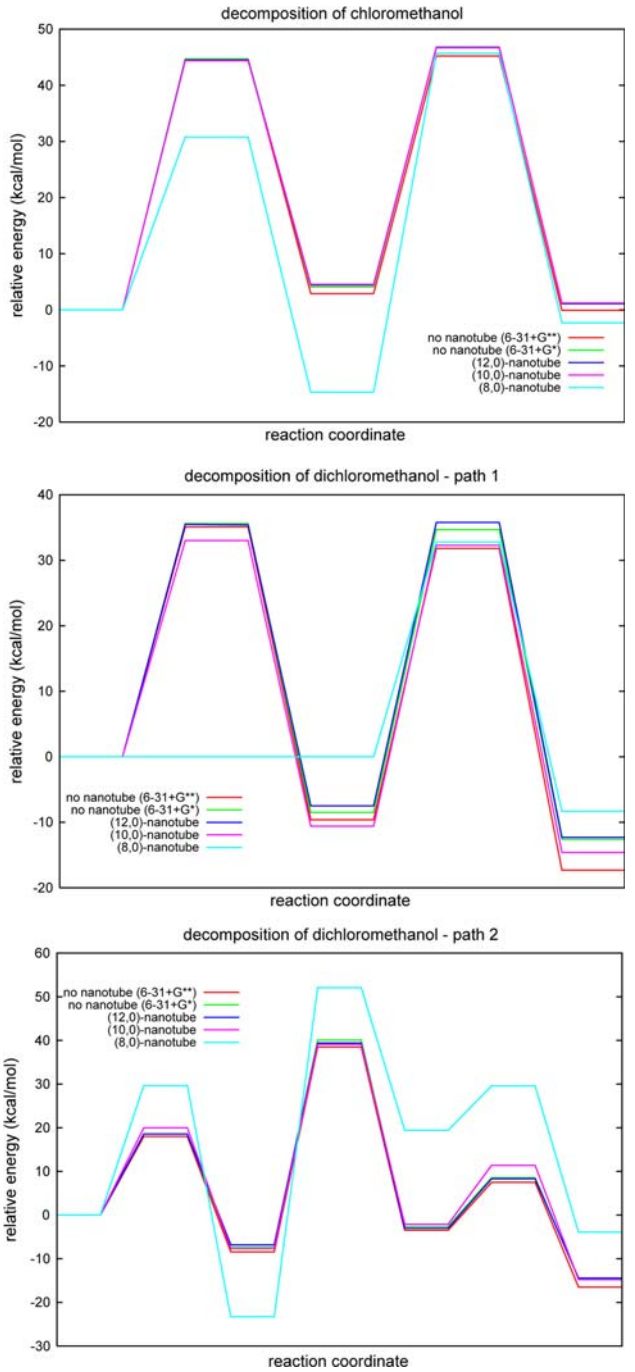

Fig. 2 Relative energy profiles of chloromethanol and dichloromethanol decomposition reactions studied in the gas phase and inside nanotubes of different sizes

3.1 Decomposition of chloromethanol

The earlier investigation of the first reaction considered here concluded that this reaction follows a two-step mechanism [12]. In the first step, a hydrogen chloride molecule is detached from the chloromethanol molecule to form a formaldehyde molecule (reaction 1). This reaction proceeds via a transition state in which the C–Cl bond is almost completely broken. The energy barrier of this reaction is estimated to be 44.7 kcal/mol and the reaction is endothermic by 4.1 kcal/mol. In the second step of the chloromethanol decomposition, the formaldehyde molecule reacts with a water molecule to form methanediol (reaction 2). This reaction is characterized by a late transition state with a

Table 1 MP2 calculated energies (ΔE, $\Delta E^{\ddagger}$), enthalpies (ΔH, $\Delta H^{\ddagger}$), free energies (ΔG, $\Delta G^{\ddagger}$)(all in kcal $mol^{-}1$) and entropies (ΔS, $\Delta S^{\ddagger}$) (in cal $mol^{-}1$ $K^{-}1$) of decomposition reactions investigated in this work

Reaction	$\Delta E^{\ddagger a}$	$\Delta H^{\ddagger a}$	$\Delta G^{\ddagger a}$	$\Delta S^{\ddagger a}$	ΔE^{b}	ΔH^{b}	ΔG^{b}	ΔS^{b}
Reaction 1: $CH_2(OH)Cl \rightarrow HCHO + HCl$								
MP2/6–31+G**	44.72	44.68	44.51	0.56	2.90	4.06	0.87	10.69
MP2/6–31+G*	44.49	44.49	44.32	0.56	5.03	5.03	1.81	10.80
(12,0)-nanotube	44.40	44.35	44.19	0.53	4.46	5.42	3.01	8.10
(10,0)-nanotube	44.29	44.20	44.11	0.30	4.22	5.18	2.68	8.40
(8,0)-nanotube	32.31	32.40	32.12	0.93	−15.51	−15.10	−16.01	3.05
Reaction 2: $HCHO + H_2O \rightarrow CH_2OH_2$								
MP2/6–31+G**	42.28	40.65	44.61	−13.30	−3.01	−4.53	−0.72	−12.78
MP2/6–31+G*	40.99	40.99	45.10	−13.77	−4.38	−4.38	−0.42	−13.29
(12,0)-nanotube	42.25	40.56	44.08	−11.78	−3.38	−4.77	−1.40	−11.30
(10,0)-nanotube	42.10	40.61	44.14	−11.86	−3.10	−4.41	−1.17	−10.88
(8,0)-nanotube	60.07	59.07	62.46	−11.37	12.95	11.87	15.44	−11.99
Reaction 3: $CH(OH)Cl_2 \rightarrow ClCHO + HCl$								
MP2/6–31+G**	37.86	37.84	37.62	0.74	−6.86	−5.59	−9.78	14.07
MP2/6–31+G*	35.35	35.35	35.35	−0.02	−7.55	−7.55	−11.54	13.38
(12,0)-nanotube	35.19	35.06	35.07	−0.05	−7.39	−6.42	−9.38	9.90
(10,0)-nanotube	33.04	32.85	33.03	−0.59	−10.88	−9.93	−12.99	10.29
(8,0)-nanotube	0.00	0.00	0.00	0.00	0.00	0.00	0.00	0.00
Reaction 4: $ClCHO \rightarrow CO+HCl$								
MP2/6–31+G**	41.46	41.72	41.05	2.26	−7.70	−6.41	−6.62	0.71
MP2/6–31+G*	43.35	43.35	42.65	2.45	−2.98	−2.98	−3.38	1.37
(12,0)-nanotube	43.07	43.35	42.62	2.43	−3.81	−2.66	−4.62	6.58
(10,0)-nanotube	42.56	42.86	42.09	2.59	−4.26	−3.08	−4.77	5.66
(8,0)-nanotube	31.20	31.33	31.05	0.92	−8.81	−7.75	−8.89	3.85
Reaction 5: $CH(OH)Cl_2+H_2O \rightarrow ClCHO+H_2O+HCl$								
MP2/6–31+G**	21.19	20.17	22.79	−8.79	−5.12	−4.14	−7.28	10.52
MP2/6–31+G*	17.48	17.48	19.90	−8.10	−6.69	−6.69	−9.41	9.11
(12,0)-nanotube	18.45	17.48	19.95	−8.29	−6.72	−6.08	−8.89	9.40
(10,0)-nanotube	20.11	19.72	19.77	−0.17	−8.35	−7.94	−10.59	8.89
(8,0)-nanotube	26.90	27.31	24.61	11.05	−25.23	−24.12	−27.74	12.16
Reaction 6: $ClCHO+H_2O \rightarrow CH(Cl)(OH)_2$								
MP2/6–31+G**	49.67	45.23	49.99	−15.96	4.90	3.24	7.90	−15.63
MP2/6–31+G*	45.60	45.60	50.17	−15.34	3.28	3.28	7.77	−15.05
(12,0)-nanotube	45.80	44.28	48.29	−13.43	3.67	2.24	6.15	−13.10
(10,0)-nanotube	46.62	45.07	49.55	−15.02	5.87	4.39	8.81	−14.83
(8,0)-nanotube	77.05	76.84	77.35	−1.69	44.23	44.08	44.46	−1.26
Reaction 7: $CH(Cl)(OH)_2+H_2O \rightarrow HCOOH+HCl+H_2O$								
MP2/6–31+G**	11.04	10.01	12.41	−8.03	−12.98	−12.36	−14.76	8.05
MP2/6–31+G*	10.21	10.21	12.32	−7.09	−11.53	−11.53	−13.88	7.86
(12,0)-nanotube	10.96	10.09	12.20	−7.10	−11.47	−10.93	−13.23	7.72
(10,0)-nanotube	12.97	12.60	12.84	−0.79	−13.35	−13.70	−13.73	7.70
(8,0)-nanotube	7.20	6.72	6.21	4.85	−24.77	−24.72	−25.91	4.01

[a] Energies, enthalpies, free energies and entropies of reactions activation

[b] Relative energies, enthalpies, free energies and entropies of reactions

short C–O bond of 1.68 Å. The energy barrier for this second reaction is also relatively high (42.3 kcal/mol), but the reaction is slightly exothermic by −3.0 kcal/mol. These results suggest that the reaction is highly unlikely to take place in the gas phase due to very large enthalpies of activation in both cases. The energy barrier of the first reaction

Table 2 MP2 calculated, non-relative energies (E) and free energies (G) (all in Hartree) of the substrates, transition states and products of the decomposition reactions investigated in this work

Reaction	Reactants		Transition states		Products	
	E	G	E	G	E	G
Reaction 1: $CH_2(OH)Cl \rightarrow HCHO + HCl$						
MP2/6–31+G*	−574.346	−574.376	−574.276	−574.305	−574.338	−574.373
(12,0)-nanotube	−574.350	−574.376	−574.279	−574.305	−574.343	−574.371
(10,0)-nanotube	−574.349	−574.375	−574.279	−574.305	−574.343	−574.371
(8,0)-nanotube	−574.315	−574.341	−574.264	−574.290	−574.340	−574.366
Reaction 2: $HCHO+H_2O \rightarrow CH_2OH_2$						
MP2/6–31+G*	−190.339	−190.374	−190.273	−190.302	−190.346	−190.374
(12,0)-nanotube	−190.344	−190.372	−190.277	−190.302	−190.349	−190.374
(10,0)-nanotube	−190.344	−190.372	−190.277	−190.301	−190.349	−190.374
(8,0)-nanotube	−190.339	−190.367	−190.243	−190.268	−190.318	−190.343
Reaction 3: $CH(OH)Cl_2 \rightarrow ClCHO + HCl$						
MP2/6–31+G*	−1,033.381	−1,033.414	−1,033.325	−1,033.358	−1,033.393	−1,033.432
(12,0)-nanotube	−1,033.385	−1,033.414	−1,033.329	−1,033.358	−1,033.397	−1,033.429
(10,0)-nanotube	−1,033.380	−1,033.409	−1,033.328	−1,033.356	−1,033.398	−1,033.429
(8,0)-nanotube	–	–	–	–	−1,033.389	−1,033.418
Reaction 4: $ClCHO \rightarrow CO + HCl$						
MP2/6–31+G*	−573.204	−573.232	−573.135	−573.164	−573.209	−573.238
(12,0)-nanotube	−573.207	−573.232	−573.138	−573.164	−573.213	−573.240
(10,0)-nanotube	−573.206	−573.231	−573.138	−573.164	−573.213	−573.239
(8,0)-nanotube	−573.199	−573.224	−573.149	−573.174	−573.213	−573.238
Reaction 5: $CH(OH)Cl_2 + H_2O \rightarrow ClCHO + H_2O + HCl$						
MP2/6–31+G*	−1,109.581	−1,109.623	−1,109.553	−1,109.591	−1,109.591	−1,109.638
(12,0)-nanotube	−1,109.589	−1,109.622	−1,109.559	−1,109.591	−1,109.599	−1,109.637
(10,0)-nanotube	−1,109.583	−1,109.615	−1,109.551	−1,109.583	−1,109.596	−1,109.631
(8,0)-nanotube	−1,109.540	−1,109.569	−1,109.497	−1,109.530	−1,109.580	−1,109.613
Reaction 6: $ClCHO + H_2O \rightarrow CH(Cl)(OH)_2$						
MP2/6–31+G*	−649.395	−649.434	−649.323	−649.354	−649.390	−649.422
(12,0)-nanotube	−649.400	−649.431	−649.327	−649.354	−649.394	−649.421
(10,0)-nanotube	−649.400	−649.432	−649.326	−649.353	−649.391	−649.418
(8,0)-nanotube	−649.393	−649.421	−649.271	−649.298	−649.323	−649.350
Reaction 7: $CH(Cl)(OH)_2 + H_2O \rightarrow HCOOH + HCl + H_2O$						
MP2/6–31+G*	−725.591	−725.631	−725.574	−725.612	−725.609	−725.653
(12,0)-nanotube	−725.598	−725.631	−725.581	−725.612	−725.617	−725.652
(10,0)-nanotube	−725.593	−725.624	−725.572	−725.604	−725.614	−725.646
(8,0)-nanotube	−725.536	−725.566	−725.525	−725.556	−725.576	−725.607

of chloromethanol decomposition may be efficiently lowered by the addition of water molecules. In the case of five or six water molecules (which correspond to almost full solvation of the system), the energy barrier is lowered drastically to only 5.6–6.6 kcal/mol [12]. For the second reaction, the addition of water molecules lowers the energy barrier, but to a lesser extent; here the addition of four H_2O molecules lowers the barrier by $\sim$15 kcal/mol [12].

The change of the basis set from 6–31+G** to 6–31+G* has almost no impact on the relative energies of the minima and the saddle points for this reaction (Fig. 2). The largest difference in the relative energies of these species is equal to $\sim$1.2 kcal/mol and is found for the products of the first step. Interestingly, the first step of this mechanism is also identical to the case of the reaction taking place inside the (12,0)-nanotube or the (10,0)-nanotube. In those two cases, the maximum difference between the energies of all minima and saddle points is smaller than 0.3 kcal/mol, suggesting that the presence of the nanotube has no impact on the course of the reaction. The small differences in the optimized bond lengths of the reactants do not exceed 0.04 Å in this case.

The situation is completely different for the system inside the smallest CNT studied in this work (Table 1). Here, the energy barrier of reaction 1 is lowered by ~12 kcal/mol to only 32.3 kcal/mol. The relative energy of the products is also lowered, which makes the reaction exothermic by −15.5 kcal/mol (as compared to the endothermic reaction in larger nanotubes and in the gas phase) (Table 1). In this case, the geometry of chloromethanol is altered due to the small size of the nanotube, which causes elongation of the C–Cl bond by 0.05 Å. Chloromethanol molecule reacts via a similar transition state leading to the C–Cl bond breaking, but the geometry of the saddle point is slightly different with the C–Cl distance equal to 2.17 Å. The geometry of the product of this reaction is, however, almost identical to the gas phase case with the O–H distance equal to 1.94 Å. There are some small differences in the orientation of the product inside the investigated nanotubes. While for the (12,0)-nanotube and the (10,0)-nanotube, the walls of the nanotubes are parallel to the C–H bond of the product, the walls of the (8,0)-nanotube are parallel to the Cl–H bond. Clearly, for large nanotubes their impact on the reactants is very weak. In contrast, for the small nanotube, the interactions of the reactants with the walls of the nanotube are relatively strong and can change the relative orientation of the whole system.

For the second step of the decomposition reaction, the results are similar. The addition of the (12,0)-nanotube or the (10,0)-nanotube to the system does not affect the outcome of the reaction (Fig. 2). If the reaction takes place in the (8,0)-nanotube, the changes in relative energies of the minima and saddle points are, however, not negligible. In this case, the energy barrier of the reaction is much higher (60.1 kcal/mol), and the reaction is endothermic by 13.0 kcal/mol (Table 1). The geometry of the formaldehyde–water complex is similar as in the gas-phase, with the intermolecular O–H distance shortened to 2.32 Å. The geometry of the transition state of this reaction is, however, completely different. The C–O distance of this transition state is equal to 1.86 Å, which is much longer than the original distance of 1.68 Å. On the other hand, one of the hydrogen atoms of the water molecule is already bonded to the oxygen atom of the formaldehyde suggesting a late transition state. The geometry of the product (methanediol) is similar to the gas phase reaction, but there is a clear difference in the O–C–O angle, which is ~112° for the gas phase case, but almost 124° inside the (8,0)-nanotube.

The noticed differences in the energetical outcome of the reactions may arise either from the stabilization/destabilization of the reactants or the stabilization/destabilization of the transition state. Results presented in Table 2 suggest that for this set of the reactions both phenomena take place. In the first step of the chloromethanol decomposition, the low energy barrier inside the (8,0)-nanotube arises from the destabilization of both the reactants and the transition state (as compared to the reaction without the nanotube). The destabilization of the reactants is, however, much larger than the destabilization of the transition state, thus resulting in the lowering of the energy barrier. Conversely, the reactants of the second step of chloromethanol decomposition have almost the same energy both within and outside the (8,0)-nanotube. In this case, the change in the energy barrier arises solely from the destabilization of the transition state structure.

A relatively large destabilization energy of the reactants is present only for the (8,0)-nanotube reactions 1, 5, and 7 (Table 2). For these three reactions, the large difference between the energy of the isolated system and the system buried within the CNT may cause the encapsulation process of the complex to be more difficult from the energetical point of view. A plausible solution to this problem may lie in adjusting the concentrations of the reactants or in applying external fields, which may make the encapsulation process easier. The latter idea has been suggested earlier by Nakatsuji et al. [26] who showed the impact of an electric field on the selected molecules. In that study, a very strong, external electric field was shown to impose changes in geometries of simple, model molecules of up to 0.04 Å (for bond lengths) and 12° (for bond angles), depending on the orientation of these molecules in the field.

3.2 Decomposition of dichloromethanol—path 1

The decomposition of dichloromethanol path comprises two reactions. The first one, analogous to the previous reaction path, is the detachment of the hydrogen chloride molecule from the dichloromethanol molecule (reaction 3). In the second step, a second HCl molecule is removed to form a CO molecule (reaction 4). Both these reactions are exothermic, by −6.9 and −7.7 kcal/mol, respectively. Both reactions also have relatively high energy barriers (37.9 and 41.5 kcal/mol, respectively), which may be lowered substantially after immersion of the system in water. In the case of adding four water molecules to the calculated system, the energy barriers were lowered in both cases to ~12 kcal/mol [12].

The energetic outcome of these two reactions is very similar when applying the smaller 6–31+G* basis set. The only large discrepancy was observed for the final product of this decomposition process, where the difference in relative energy was 3.6 kcal/mol (Table 1).

The addition of the (12,0)-nanotube has a minimal effect on the course of this reaction. If the reaction takes place in the (10,0)-nanotube, there are some differences in the relative energies of the minima and the saddle point for the first reaction. The energy barrier for this reaction is

lowered by 2.2 kcal/mol, and the reaction is more exothermic by an additional 2.4 kcal/mol (Fig. 2).

As in the previous example, the reaction inside the (8,0)-nanotube has completely different characteristics. The first reaction, in which one HCl is detached from the substrate, follows a barrierless mechanism. This result suggests that the dichloromethanol molecules are unstable inside a small CNT and, upon entering the nanotube, undergo an immediate reaction. The product of the reaction, the CHClO–HCl complex, has a much higher energy than the gas-phase product of this reaction (Fig. 2).

The second reaction of the decomposition process involves much smaller molecules, which should not be affected in such a strong way by the presence of the nanotube limiting the available space. Indeed, the results confirm this hypothesis. The geometrical parameters and the energies of the product, the transition state, and the substrate of the second reaction are similar to each other and are minimally affected by the presence of the nanotube. The biggest difference occurs, as expected, for the smaller (8,0)-nanotube. Here, the energy barrier is lowered by $\sim$12 kcal/mol while the energy of the products is lowered by 5.5 kcal/mol (Table 1). The geometries of the molecular systems are similar in all calculated cases.

3.3 Decomposition of dichloromethanol—path 2

The decomposition of dichloromethanol can also follow a different route. The mechanism involves three reactions. The first one is identical to path 1 of the dichloromethanol decomposition that produces a CHClO molecule (reaction 5). Unlike in path 1, this molecule does not undergo a second decomposition. Instead a water molecule reacts with CHClO to form chloromethanediol ($CHCl(OH)_2$) (reaction 6). In the presence of water, this compound undergoes decomposition into formyl acid and HCl in the last step of the path (reaction 7).

The impact of the use of a smaller basis set in the calculations of this reaction is marginal but not negligible. For all three reactions, the maximum discrepancy between the results obtained using 6–31+G** and 6–31+G* basis sets is equal to 4.1 kcal/mol (Table 1).

Since all three reactions in this path involve larger molecular systems than those in the previous case, one should expect a larger impact of the confined space on their mechanisms. This is indeed the case. For the first reaction of the dichloromethanol decomposition in the presence of one water molecule, the addition of the (12,0)-nanotube has a minimal impact on the energetics of the reaction (Table 1). In the case of the (10,0)-nanotube, the situation is different. Both the reactants and the transition state geometries are altered to some degree by the much more limited space available for the reaction. The product of the reaction is the same from the chemical point of view, but it forms a different linear complex. The relatively large differences in geometrical parameters have, in this case, a small impact on the energetic outcome of the reaction. The barrier of the reaction is 1.5 kcal/mol higher than in the (12,0)-nanotube case, but the energies of the reactants and the products are still almost identical.

The (8,0)-nanotube has an even larger impact on the reaction. The geometries of the reactants and the transition state-complex inside the smallest nanotube studied here are distorted to a large extent, while the geometry of the final product is completely different from the gas-phase case. In this case, however, alterations in geometries are followed by large changes in the energies of the minima and the saddle-points (Fig. 2).

The second reaction of this pathway is much less affected by the presence of the nanotubes. For the (12,0)-nanotube, both the geometries and the energies are almost identical to those in the gas phase. In the case of the (10,0)-nanotube, there are minor changes in the geometries of the reactants and the transition state complex, but the energies are not changed. When the reaction takes place inside the (8,0)-nanotube, the geometries of the system are altered to an even greater extent, as is the energetic outcome of the reaction. In this case the barrier of the reaction is much higher at $\sim$77 kcal/mol, and the reaction is endothermic by approximately 44 kcal/mol (Table 1).

A very similar pattern of system behavior may be observed for the third and the last reactions of this pathway. The impact of the (12,0)-nanotube on both the geometries and on the energetics of the reaction is almost negligible. The (10,0)-nanotube alters, to some extent, the geometries of the minima and the saddle point of this reaction, while keeping the energetic outcome of the reaction at the same level. The (8,0)-nanotube alters both the geometrical parameters and the energetic outcome of the reaction, making the reaction much more exothermic (Table 1).

3.4 Vibrational analysis

In the previous section, we have shown that the presence of nanotubes has, in some cases, a large impact on the geometrical parameters and the energetics of the reactants. If so, the presence of the nanotubes should also alter the vibrational modes of the reactants. We have performed a vibrational analysis of some of the reactants to describe the differences between the gas phase and confined space reactions. we will not describe all of them due to the large number of systems studied in this work. Instead, we will concentrate on one selected system, which will provide a basis for more general conclusions concerning this issue.

Table 3 Vibrational modes of the product of the first chloromethanol decomposition reaction (reaction 1) in the gas phase and encapsulated by CNTs of different diameter (in cm^{-1})

Mode	Gas phase	(12,0)-CNT	(10,0)-CNT	(8,0)-CNT
ν_1	45.5	33.9	36.2	27.4
ν_2	153.0	102.6	125.2	203.3
ν_3	166.1	168.7	183.1	209.3
ν_4	430.2	489.6	503.4	507.4
ν_5	443.0	565.2	583.2	588.8
ν_6	1,208.7	1,213.1	1,216.8	1,272.7
ν_7	1,285.5	1,288.5	1,304.5	1,355.8
ν_8	1,561.7	1,563.3	1,579.0	1,635.6
ν_9	1,748.3	1,742.3	1,751.3	1,824.8
ν_{10}	2,838.9	2,755.6	2,742.2	2,860.9
ν_{11}	3,050.1	3,052.2	3,079.2	3,315.1
ν_{12}	3,142.5	3,148.0	3,174.1	3,664.2

In Table 3, we present vibrational spectra of the product of the first reaction of the chloromethanol decomposition (reaction 1), the formaldehyde–HCl complex, obtained in the gas-phase calculations and for the system placed inside three CNTs of different diameters. It is obvious that there should be some differences in the theoretical spectra obtained for those four systems. This is indeed the case and, not surprisingly, the largest differences are present for the complex inside the smallest nanotube. In general, most of the vibrational modes are shifted towards higher frequencies for the systems inside the nanotubes. While for the (12,0)-nanotube systems these shifts are relatively small (usually 2–10 cm^{-1}), the shifts for the (10,0)-nanotube systems are much larger (usually in the range of 10–30 cm^{-1}). In the case of the (8,0)-nanotube, the vibrational modes are even more shifted (ranging from 50 to 300 cm^{-1}).

It is also interesting to notice that, in all cases of the reactants inside the nanotubes, there are additional vibrational modes corresponding to the nanotube–reactant interaction. These modes usually present in the 0–100 cm^{-1} region correspond to the reactant's "bouncing" modes. These types of vibrational modes are unique to the systems encapsulated by CNTs.

The results, suggesting the small shifts of vibrational modes towards higher frequencies, are in good agreement with the recent results obtained for fullerene–nanotube complexes using the SCC-DFTB-D method [27]. Unfortunately, most of the shifts of the vibrational modes are relatively weak, while stronger shifts are present mostly in the 0–500 cm^{-1} range, which is difficult to access by the experimental techniques. This general result suggests that the experimental determination of the studied species using IR techniques may be rather difficult [27].

4 Conclusions

The effects of the confinement of chloromethane and dichloromethane decomposition reactions inside CNTs with different diameters have been studied in this work using a combination of ab initio and molecular mechanics techniques. A nanotube with a large diameter (as compared to the size of the reactants) has an almost negligible effect on the course of the reaction. On the other hand, a small nanotube with a diameter similar to the size of the reactants, usually has a large impact on the reaction. The results obtained in this work suggest that the encapsulation by nanotubes significantly reduces the reaction barriers and the overall endothermicity of the decomposition reactions. Conversely, in the case of synthesis reactions, the expected effect of the confinement inside nanotubes is an increase of the energy barrier and an increase of the endothermicity of the reaction.

The effect of the confinement may be relatively large (in some cases even preventing the reaction to occur) or it can make the reaction barrierless. It is interesting to note that this effect should occur for any reactions taking place in a confined space, and not just those reactions occurring inside nanotubes. The present results may allow us to develop the means to better control chemical reactions in different environments. Unfortunately, in the case of more complex reactions, the impact of the confinement on the reaction is more difficult to predict. In such cases theoretical calculations, such as those presented in this work, may present a viable alternative.

The results presented in this work suggest that differences in entropy between reactions in the gas-phase and for confined systems are relatively small. However, encapsulation by CNTs has a relatively large influence on the geometrical parameters of the reactants. Structural changes forced by the confinement of the nanotube have, in turn, a large impact on the energies and enthalpies of the reactants, altering the energy barriers and the energetic outcomes of the reactions.

Another effect of the nanotube encapsulation is a change in the vibrational spectrum of the reactants. In most cases, the vibrational frequencies corresponding to the reactants are shifted in comparison to the gas-phase spectra. The shifts depend on the structural distortions, and those are directly related to the size of the nanotube. Additionally, new modes resulting from the reactants–nanotube interactions appear in the spectrum. Unfortunately, theoretical results presented in this investigation suggest that changes in the geometry upon encapsulation may not be visible in the experimental IR spectrum of the molecules.

Acknowledgments CPU time from the University of Arizona supercomputing center is gratefully acknowledged. Figures 1 and 3–9

were created using the xyzviewer software written by Sven de Marothy. We thank Abraham F. Jalbout for helpful suggestions concerning this work.

References

1. Britz DA, Khlobystov AN, Porfyrakis K, Ardavan A, Briggs GAD (2005) Chem Commun 37
2. Pichler T, Kuzmany H, Kataura H, Achiba Y (2001) Phys Rev Lett 87:267401
3. Pan X, Bao X (2008) Chem Commun 6271
4. Halls MD, Schlegel HB (2002) J Phys Chem B 106:1921
5. Lu T, Goldfield EM, Gray SK (2008) J Phys Chem C 112:2654
6. Lu T, Goldfield EM, Gray SK (2008) J Phys Chem C 112:15260
7. Yuan S, Wang X, Li P, Li F, Yuan S (2008) J Appl Phys 104:054310
8. Barajas-Barraza RE, Ramirez-Ruiz JA, Guirado-Lopez RA (2008) J Comput Chem Nanosci 5:2255
9. Bianco A, Kostarelos K, Prato M (2005) Curr Opin Chem Biol 9:674
10. Tyndall GS, Wallington TJ, Hurley MD, Schneider WF (1993) J Phys Chem 97:1576
11. Wallington TJ, Schneider WF, Barnes I, Becker KH, Sehested J, Nielsen OJ (2000) Chem Phys 322:97
12. Phillips DL, Zhao C, Wang D (2005) J Phys Chem A 109:9653
13. Scheytt H, Esrom H, Prager L, Mehnert R, von Sonntag C (1993) Non-thermal plasma techniques for pollution control, Part B. In: Penetrant BM, Schultheis SE (eds) NATO ASI series G 34 B, electron beam and electrical discharge processing. Springer, Heidelberg
14. von Sonntag C, Mark G, Mertens R, Schuchmann MN, Schuchmann HP (1993) J Water Supply Res Technol Aqua 42:201
15. Mertens R, von Sonntag C (1994) Angew Chem Int Ed Engl 33:1259
16. Mertens R, von Sonntag C (1994) J Chem Soc Perkins Trans 2:2181
17. von Sonntag C, Schuchmann HP (1994) Methods Enzymol 233:3
18. Dowideit P, Mertens R, von Sonntag C (1996) J Am Chem Soc 118:11288
19. Møller C, Plesset MS (1934) Phys Rev 46:618
20. Maseras F, Morokuma K (1995) J Comp Chem 16:1170
21. Dapprich S, Komáromi I, Byun KS, Morokuma K, Frisch MJ (1999) J Mol Struct THEOCHEM 461–462, 1
22. Rappé AK, Casewit CJ, Colwell KS, Goddard III WA, Skiff WM (1992) J Am Chem Soc 114:10024
23. Basiuk VA (2003) J Phys Chem B 107:8890
24. Basiuk VA (2004) J Nanosci Nanotech 4:1095
25. Gaussian 03 Revision C.02 Frisch MJ, Trucks GW, Schlegel HB, Scuseria GE, Robb MA, Cheeseman JR, Montgomery JA Jr, Vreven T, Kudin KN, Burant JC , Millam JM, Iyengar SS, Tomasi J, Barone V, Mennucci B, Cossi M, Scalmani G, Rega N, Petersson GA, Nakatsuji H, Hada M, Ehara M, Toyota K, Fukuda R, Hasegawa J, Ishida M, Nakajima T, Honda Y, Kitao O, Nakai H, Klene M, Li X, Knox JE, Hratchian HP, Cross JB, Bakken V, Adamo C, Jaramillo J, Gomperts R, Stratmann RE, Yazyev O, Austin AJ, Cammi R, Pomelli C, Ochterski JW, Ayala PY, Morokuma K, Voth GA, Salvador P, Dannenberg JJ, Zakrzewski VG, Dapprich S, Daniels AD, Strain MC, Farkas O, Malick DK, Rabuck AD, Raghavachari K, Foresman JB, Ortiz JV, Cui Q, Baboul AG, Clifford S, Cioslowski J, Stefanov BB, Liu G, Liashenko A, Piskorz P, Komaromi I, Martin RL, Fox DJ, Keith T, Al-Laham MA, Peng CY, Nanayakkara A, Challacombe M, Gill PMW, Johnson B, Chen W, Wong MW, Gonzalez C, Pople JA, Gaussian Inc Wallingford CT (2004)
26. Nakatsuji H, Hayakawa T, Yonezawa T (1981) J Am Chem Soc 103:7426
27. Witek H, Trzaskowski B, Małolepsza E, Morokuma K, Adamowicz L (2007) Chem Phys Lett 446:87